Available online at www.sciencedirect.com
SCIENCE DIRECT®
PERGAMON
Chaos, Solitons and Fractals 19 (2004) 285–291
CHAOS SOLITONS & FRACTALS
www.elsevier.com/locate/chaos

Fractal dimensional analysis of Indian climatic dynamics

Govindan Rangarajan [a,*], Dhananjay A. Sant [b]

[a] Department of Mathematics and Centre for Theoretical Studies, Indian Institute of Science, Bangalore 560 012, India
[b] Department of Geology, Faculty of Science, M.S. University of Baroda, Vadodara 390 002, India

Abstract

In this paper, we use fractal dimensional analysis to investigate the Indian climatic dynamics. We analyze time series data of three major dynamic components of the climate—temperature, pressure and precipitation. We study how climate variability changes from month to month and from one season to the other. We also investigate variability both at a local level (for individual stations) and at a regional level (for groups of stations). Our studies suggest that regional climatic models typically would not be able to predict local climate since they deal with averaged quantities. We find an interesting effect that precipitation during the south-west monsoon is affected by temperature and pressure variability during the preceding winter.

1. Introduction

Fractal dimensional analysis of geophysical time series is a well established investigative tool for exploring the dynamics. This was initiated by Mandelbrot and Wallis in their series of seminal papers [1–3] on this subject. This has been followed up by application of the technique to various geophysical phenomena [4–6]. Fractal dimensional analysis is particularly well suited to analyze the variability of a given time series. In this paper we concentrate on investigating the Indian climatic dynamics through an analysis of the temperature, pressure and precipitation time series. As these three variables form the dominant dynamic component of climate, our emphasis on them is well justified. Since the Indian subcontinent lies at the heart of the classic monsoon region and is the area most sensitive to monsoon fluctuations, fractal dimensional analysis of its climatic time series can be expected to yield some insights into how the Indian climate variability is linked to monsoon fluctuations.

In a previous paper [7], using fractal dimensional analysis, we had introduced the concept of a climate predictability index as a tool for studying climate dynamics and briefly explored its applications. In this paper, we undertake a detailed analysis of the Indian climate dynamics using the predictability indices as the main tool. Predictability indices are calculated for 31 recording stations spread throughout India. These indices are computed using temperature, pressure and precipitation time series data for these stations available from the global historical climatology network (GHCN) dataset [8]. We calculate these indices both for a season as a whole and for individual months. This enables us to study the climate dynamics at two temporal resolutions. Next, we study individual stations as well as groups of stations. This allows us to identify both local dynamics as well as regional dynamics.

2. Fractal dimensional analysis

We start with the assumption that climatic time series can be modeled as a stationary stochastic process. Consider a stationary stochastic process in discrete time, $\{\xi_k\}$, with $\langle \xi_k \rangle = 0$ and $\langle \xi_k^2 \rangle = \sigma^2$. Here $\langle\ \rangle$ denotes ensemble average. If the autocorrelation function $C(n) = \langle \xi_k \xi_{k+n} \rangle$ scales with the lag n as

* Corresponding author.
E-mail address: rangaraj@math.iisc.ernet.in (G. Rangarajan).

0960-0779/03/$ - see front matter
doi:10.1016/S0960-0779(03)00042-0

$$C(n) \sim n^{-\beta} \tag{2.1}$$

for large n, where $0 < \beta < 1$, then $\{\xi_i\}$ is called a long range correlated or long memory process [9]. The reason for the latter term is that $C(n)$ decays so slowly that $\sum_{n=1}^{N} C(n)$ diverges as $N \to \infty$. It is well known [1,4–6,10] that most geophysical time series and in particular the climatic time series that we wish to analyze exhibit this long memory property.

A standard method to assess the correlation structure of $\{\xi_k\}$ is to convert the stationary process to a random walk by using partial sums, $R_1 = \xi_1, R_2 = \xi_1 + \xi_2, \ldots, R_n = \xi_1 + \xi_2 + \cdots + \xi_n, \ldots$, where R_n is the position of the walker at time n. The mean range of the random walk trajectory as a function of time bears specific relations with the scaling relation Eq. (2.1). For ease of analytical evaluation we consider the mean square displacement as a measure of the range of the random walk, which is defined as

$$\langle R_n^2 \rangle = \sum_{i=1}^{n} \langle \xi_i^2 \rangle + 2 \sum_{s=1}^{n-1} (n-s) C(s) = n\sigma^2 + 2n \sum_{s=1}^{n-1} C(s) - 2 \sum_{s=1}^{n-1} sC(s). \tag{2.2}$$

Let $C(s)$ obey the scaling law in Eq. (2.1). The sums in the above equation are estimated as

$$\sum_{s=1}^{n-1} C(s) \sim \sum_{s=1}^{n} s^{-\beta} \sim \int_1^n s^{-\beta} \sim n^{1-\beta} \tag{2.3}$$

and

$$\sum_{s=1}^{n-1} sC(s) \sim \sum_{s=1}^{n} s^{1-\beta} \sim \int_1^n s^{1-\beta} \approx n^{2-\beta}. \tag{2.4}$$

For $0 < \beta < 1$ this means

$$\langle R_n^2 \rangle \sim n^{2-\beta} \tag{2.5}$$

for large n. Conventionally, the mean square displacement is characterized by the Hurst exponent H as

$$\langle R_n^2 \rangle \sim n^{2H}, \tag{2.6}$$

where

$$H = (2 - \beta)/2. \tag{2.7}$$

The random walk analysis tool that we will use in this paper is the rescaled range (R/S) analysis [1,10]. A brief description of this method follows. For a given dataset $\{\xi_i\}$, consider the sum $L(n,s) = \sum_{i=1}^{s} \xi_{n+i}$, where $L(n,s)$ can be regarded as the position of a random walk after s steps. Define the trend-corrected range $R(n,s)$ of the random walk as

$$R(n,s) = \max\{L(n,p) - pL(n,s)/s, 1 \leqslant p \leqslant s\} - \min\{L(n,p) - pL(n,s)/s, 1 \leqslant p \leqslant s\}. \tag{2.8}$$

Let $S^2(n,s)$ denote the variance of the dataset $\{\xi_{n+i}\}_{i=1}^{s}$. If the data has long range correlation, the average rescaled statistic $Q(s) = \langle R(n,s)/S(n,s) \rangle_n$ (where $\langle \rangle_n$ denotes the average over n) scales with s as a power law for large s:

$$Q(s) \sim s^H, \tag{2.9}$$

where H is the Hurst exponent introduced earlier. This power law manifests itself as a straight line in the log–log plot of $Q(s)$ vs. s.

The Hurst exponent is related to the fractal dimension D of the time series curve by the formula [11]

$$D = 2 - H. \tag{2.10}$$

If the fractal dimension D for the time series is 1.5, there is no correlation between amplitude changes corresponding to two successive time intervals. Therefore, no trend in amplitude can be discerned from the time series and hence the process is unpredictable. However, as the fractal dimension decreases to 1, the process becomes more and more predictable as it exhibits "persistence". That is, the future trend is more and more likely to follow an established trend [5]. As the fractal dimension increases from 1.5 to 2, the process exhibits "anti-persistence". That is, a decrease in the amplitude of the process is more likely to lead to an increase in the future. Hence, the predictability again increases. However, we will be concerned only with persistence behaviour since all geophysical time record analyzed till date [1,4–6,10] exhibit this behaviour.

Table 1
Climate predictability index (PI_C) for 15 stations spread throughout India

Station	SW	NE
Allahabad	(0.2,0.8,0.1)	(0.6,0.2,0.0)
Bangalore	(0.3,0.3,0.2)	(0.5,0.1,0.1)
Bombay	(0.5,0.7,0.5)	(0.5,0.7,0.2)
Calcutta	(0.9,0.7,0.2)	(0.9,0.0,0.4)
Darjeeling	(0.5,0.7,0.4)	(0.6,0.7,0.1)
Dwaraka	(0.3,0.2,0.2)	(0.1,0.2,0.2)
Gauhati	(0.5,0.4,0.1)	(0.4,0.1,0.0)
Hyderabad	(0.7,0.7,0.3)	(0.8,0.5,0.2)
Kodaikanal	(0.9,0.8,0.1)	(0.6,0.8,0.3)
Madras	(0.6,0.8,0.4)	(0.1,0.7,0.0)
Nagpur	(0.2,0.6,0.4)	(0.2,0.2,0.0)
New Delhi	(0.5,0.7,0.3)	(0.3,0.7,0.4)
Shillong	(0.5,0.2,0.5)	(0.3,0.0,0.0)
Simla	(0.8,0.2,0.2)	(0.5,0.2,0.1)
Veraval	(0.9,0.4,0.6)	(0.4,0.4,0.1)

PI_C is listed for two seasons—the south-west and north-east monsoon periods.

We obtain the fractal dimensions of the time series corresponding to temperature, pressure and precipitation for a given location using R/S analysis to first obtain H and then Eq. (2.10). The fractal dimensions are denoted by D_T, D_P and D_R respectively. The R/S analysis is used merely because it has been the conventional technique used for geophysical time records [1,4–6,10]. Any other method would be equally adequate.

Predictability indices (denoted by PI_T, PI_P and PI_R respectively) for temperature, pressure and precipitation are defined as follows [7]:

$$PI_T = 2|D_T - 1.5|; \quad PI_P = 2|D_P - 1.5|; \quad PI_R = 2|D_R - 1.5|.$$

Here $|D|$ denotes the absolute value of the number D. We use absolute values since predictability increases in both the following cases—when the fractal dimension becomes less that 1.5 and when it becomes greater than 1.5. In the former case, we have correlation (persistence) behaviour and in the latter case, anti-correlation (anti-persistence) behaviour. However, in either case, the process becomes more predictable. Thus, use of absolute values ensures that a process with $D = 1.3$ has the same predictability index as a process with $D = 1.7$.

The climate predictability index (PI_C) is defined as the collection of the above three indices:

$$PI_C = (PI_T, PI_P, PI_R).$$

If one of these indices is close to zero, then the corresponding process approximates the usual Brownian motion and is therefore unpredictable. If it is close to one, the process is very predictable. Note that the PI_R value is not related to the amount of precipitation, but to how precipitation changes from year to year. The rationale for introducing the climate predictability index is as follows. In this paper, we are interested in studying the inter-relationships between the three climatic components from the viewpoint of fractal dimensions. Hence, it is useful to have all three of them represented in a single index. Then it is easier to see how the three sub-indices change in relation to one another as the seasons change. Further, by introducing predictability indices instead of fractal dimensions, we focus on how predictable the process is. This is especially useful for precipitation.

Data from 31 measuring stations spread throughout India were studied. The temperature, pressure and precipitation time series for these stations were obtained from the GHCN dataset [8]. The dataset gives monthly mean values for the above three climatic variables. Mean values for various seasons were obtained by averaging over the months constituting the season under study. These time series data were then studied using R/S analysis and predictability indices calculated using the formulas given above.

Table 1 gives the predictability indices for temperature, pressure and precipitation respectively for a few representative stations. Predictability indices are listed for two seasons—south-west monsoon, north-east monsoon.

3. Data analysis

We now study how the predictability indices change with the seasons and within the seasons. We concentrate on the following seasons—pre-south-west monsoon season (March–May), south-west monsoon season (June–September) and

north-east monsoon season (October and November). Each of these seasons is studied separately below. Four stations exhibit a consistent predictability pattern across the seasons. We list them first before going into a season-wise analysis. Calcutta has a predictable temperature whereas Darjeeling, Hyderabad and Kodaikanal have a predictable pressure throughout the year.

3.1. Pre-south-west monsoon season

First, we consider predictability indices calculated for this season as a whole. Fig. 1 gives the scatter plot of PI_T vs. PI_P for this season. We see that the stations are equally distributed across all regions of the graph. Roughly, one-third of the stations have unpredictable PI_T and PI_P. Even if one considers only those stations (concentrated mainly in the north-eastern region) where it rains significantly during this season, they do not exhibit any consistent behaviour as far as PI_T and PI_P are concerned. This shows that local factors play an important role and further detailed studies are required. Predictability index for precipitation was not studied since a majority of the stations do not get significant rainfall during this season.

Next, we consider how the predictability indices change with the months (viz. March, April and May) constituting this season. We observe that all coastal stations (with the exception of Dwaraka) have predictable temperature during each month. However, pressure is not predictable for all months for these stations. For central Indian stations, temperature is not predictable. For north-eastern stations, pressure is not predictable.

3.2. South-west monsoon season

If one looks at the seasonal values of the predictability indices, the following regional patterns are observed. The coastal and north-eastern stations have predictable temperature (again with the exception of Dwaraka). Stations situated in the core of the Indian monsoon (centered around Central India) have unpredictable temperature whereas pressure is predictable. For these stations, the variability in precipitation is linked to the variability in temperature.

As for PI_R, nine stations have reasonably high predictability (greater than or equal to 0.5) if one looks at the south-west monsoon season (June–September) as a whole. However, if one looks at PI_R for the individual months constituting the season, no station has high predictability for all these months. This anomaly can be explained as follows. It is quite possible that the total rainfall for the season follows a more consistent pattern across the years as compared to the rainfall in individual months. The monthly rainfall could be more unpredictable because of delays in onset of monsoon for that station etc. whereas even a delayed monsoon can give the same amount of rainfall for the entire season as compared to a normal monsoon. The difference between the seasonal PI_R and monthly PI_R quantifies this for each

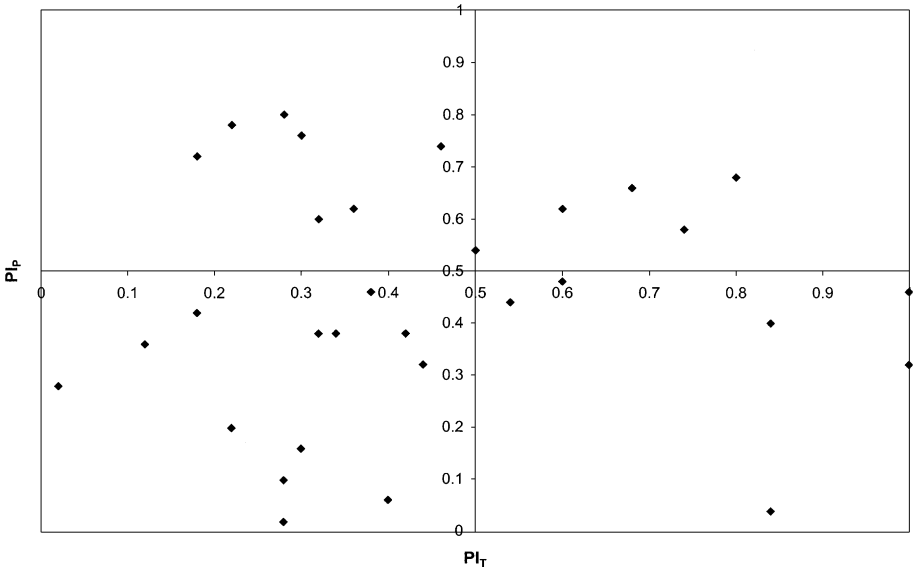

Fig. 1. Scatter plot of PI_T vs. PI_P for the pre-south-west monsoon season (March–May).

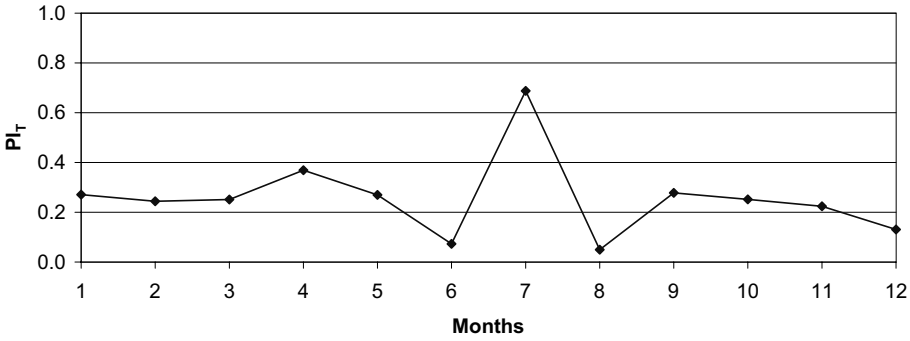

Fig. 2. Temperature predictability graph for Nagpur showing the variation of the monthly PI_T values with the months.

station. Also note that PI_R is not directly related to the amount of rainfall. It only measures the predictability of the rainfall.

Next, we looked for correlations between the south-west monsoon rainfall and the various monthly predictability indices. Correlations were calculated using data from all stations except those which have a long rainy season (stretching from March/April to October/November). Significant positive correlations of the south-west monsoon rainfall (significant at the 5% level) were observed with both February PI_T and March PI_P. This suggests that the temperature/pressure dynamics during the February–March period (the transition period between winter and summer) prior to the monsoon could play a role in the south-west monsoon rainfall over the Indian subcontinent.

Next, we looked for characteristic patterns in the temperature and pressure predictability graphs (i.e. graphs of PI_T and PI_P as a function of months) for a given station prior to the onset of the south-west monsoon. An example of such a graph is given in Fig. 2 for Nagpur. No pattern was observed in the pressure predictability graphs. On the other hand, the temperature predictability graphs for stations getting significant rainfall (greater than 10 cm monthly) during the south-west monsoon exhibited a characteristic dip prior to the onset of the monsoon. However, there were a few exceptions. Stations at high elevations did not exhibit this pattern which is understandable since such stations typically have a quite different climatic dynamics. The other exceptions were Veraval (situated along the West coast) and New Delhi where other local/geographical factors probably play a role.

3.3. North-eastern monsoon season

We now study the regional distribution of PI_T and PI_P for the north-east monsoon season (October–November). We first consider stations in the southern and eastern India where it rains significantly during the north-east monsoon. The north-eastern region where it rains practically throughout the year appears to have a different dynamics dictated by local geographical factors. However, other stations exhibit the following patterns in the predictability indices calculated for this season. Rainfall is unpredictable for all stations. Except for three stations (considered separately below), temperature is predictable whereas pressure is unpredictable. Therefore, it is the variability in pressure which causes the rainfall unpredictability.

The two high elevation stations (Kodaikanal and Darjeeling) follow a different pattern. Both their temperature and pressure are predictable whereas rainfall is unpredictable. Here, their elevation seems to play a role. The other exception is Madras. Here temperature is unpredictable whereas pressure is predictable. This is in contrast to what is observed for other stations. One interesting fact (which may be related to this contrary behaviour) is that Madras alone of all these stations gets its maximum rainfall during the month of November rather than October.

4. Discussions

Most climatic studies deal with a region or a season as a whole. Even predictions for the Indian monsoon deal with the whole subcontinent. However, for (say) a farmer at a specific location, the only thing which matters is whether rainfall is good at her/his location in a given month. In our paper, we have therefore studied predictability of the climate at two temporal scales—for the season as a whole and for individual months within the season. We find that even if the seasonal rainfall is predictable at a given location, the monthly rainfall is not. For individual stations spread throughout

the Indian subcontinent, our studies quantify the discrepancy between predictability of seasonal vs. monthly rainfall and consequently the limitations of gross climatic models.

We have also investigated whether regional patterns exist for the predictability indices. We have found some patterns (detailed in the previous section). But these patterns exist only for sub-regions of the Indian subcontinent and not for the whole subcontinent. This again highlights the fact that even if monsoon rainfall is predicted to be good for the whole subcontinent using a regional climatic model that averages over the entire region, individual regions may be hit with drought/flood. Therefore, regional climatic models typically do not predict such local extreme events since they deal with averaged quantities. We extend this analogy to paleoclimatic data from the continents, where data largely represents climate of short-lived local depositional events [12,13] and does not represent the overall climate of the region. This shows that the link between regional climate and paleoclimatic data is weak. However strong events that influence fundamental processes do get recorded as climatic events with a time lag. The lag depends on how climate change influences the site and dynamics of the proxies at the site.

Our observations in the previous section also support the well known fact that climate is a very complex system. However, this complexity has been studied from a different viewpoint in this paper using predictability indices. The complexity is manifest in the absence of any strong regional vs. local and seasonal vs. monthly correlations in the predictability indices.

In this paper, we have also extended the analysis carried out in our previous paper [7] for the south-west monsoon. There we had studied stations with low predictability for rainfall and analyzed causes for the same. In this paper, the same analysis was performed for the north-east monsoon. We found that for most stations it is the unpredictability in pressure which leads to the unpredictability in rainfall.

We also find that the dynamics of the south-west monsoon is affected by the transition from winter to summer in the previous February–March period. This corresponds to the observation [12,14] that in years of weak glacial/low snowfall (weak winter over the continent), the Tibetan plateau is able to warm up earlier leading to a strong monsoon. On the other hand, a delayed or weak monsoon is due to deep snow (severe winter over the continent) [15]. In the core region of the monsoon, pressure is consistent across the years (leading to higher PI_P) and it is the variability in temperature that causes the variability in rainfall. However, this pattern reverses during the north-east monsoon. For this monsoon, there is no winter to summer like transition for temperature prior to the monsoon. Further, since it has already been raining (during the south-west monsoon) prior to this monsoon, there is a general cooling trend in temperature which makes it predictable in the core region for this monsoon (which is now centered around south-east India). On the other hand, the pressure is observed to become unpredictable leading to variability in the north-eastern monsoon rainfall.

Acknowledgements

We would like to thank Prof. N.V. Joshi for useful discussions. This work was supported by a research grant from DRDO under the Engineering Mathematics Programme at IISc. GR is also associated with the Jawaharlal Nehru Centre for Advanced Scientific Research, Bangalore as a Honorary Faculty.

References

[1] Mandelbrot BB, Wallis JR. Some long-run properties of geophysical records. Water Resour Res 1969;5:321–40.
[2] Mandelbrot BB, Wallis JR. Noah, Joseph and operational hydrology. Water Resour Res 1968;4:909–18.
[3] Mandelbrot BB, Van Ness JW. Fractional Brownian motions, fractional noises and applications. SIAM Rev 1968;10:422–37.
[4] Flugeman Jr RH, Snow RS. Fractal analysis of long-range paleoclimatic data: oxygen isotope record of Pacific core V28–239. Pure Appl Geophys 1989;131:307–13.
[5] Hsui AT, Rust KA, Klein GD. A fractal analysis of Quarternary, Cenozoic–Mesozoic, and Late Pennsylvanian sea level changes. J Geophys Res 1993;98B:21963–7.
[6] Turcotte DL. Fractals and chaos in geology and geophysics. New York: Cambridge University Press; 1992.
[7] Rangarajan G, Sant DA. A climate predictability index and its applications. Geophys Res Lett 1997;24:1239–42.
[8] Vose, RS et al. The global historical climatology network: long-term monthly temperature, precipitation, sea level pressure, and station pressure data. National Oceanic and Atmospheric Administration, Asheville, 1995.
[9] Beran J. Statistics for long-memory processes. New York: Chapman & Hall; 1994.
[10] Hurst HE, Black RP, Simaika YM. Long-term storage: an experimental study. London: Constable; 1965.
[11] Voss RF. In: Pynn R, Skjeltorp A, editors. Scaling phenomena in disordered systems. New York: Plenum; 1985.
[12] Overpeck J, Anderson D, Trumbore S, Prell W. The south-west Indian monsoon over the last 18000 years. Climate Dyn 1996;12:213–25.

[13] Sirocko F, Sarnthein M, Erlenkeuser H, Lang H, Arnold M, Duplessy JC. Century-scale events in monsoonal climate over past 24000 years. Nature 1993;364:322–4.
[14] Van Campo E, Duplessy JC, Rossignol-Strick M. Climatic conditions deduced from a 150 Kyr oxygen-isotope-pollen record from the Arabian sea. Nature 1982;296:56–9.
[15] Barnett TP, Dumenil L, Schlese U, Roeckner E, Latif M. The effect of Eurasian snow cover on regional and global climate variations. J Atmos Sci 1989;46:661–8.